computerized tomography profile of the olfactory fossa based on keros classification and the anterior ethmoid artery location to the skull base

Doaa Faris Jabaz* , Raad Hefdhi Abedtwfeq**

*** Department of Surgery/College of Medicine, AL-Qadisiyah University**
**** President of the Iraqi society of radiology and Medical Imaging**

Abstract

Anatomical variations in olfactory fossa depth and anterior ethmoid arteries (AEAs) course are of great importance during functional endoscopic sinus surgery (FESS) as they may result in iatrogenic damages thus surgical planning is tailored with the aid of a CT scan preoperatively. This study was conducted to assess the olfactory fossae depth according to Keros classification and to localize the course of AEAs in Iraqi patients using computerized tomography, a probable relationship between olfactory fossae depth and AEA location was assessed. A cross-sectional observational study involved 189 adult patients (99 females and 90 males) referred to our radiology department for evaluation of paranasal sinus. Patients were examined by the same CT device, excluding those with altered anatomy due to trauma, aggressive inflammation, or tumor and those less than 18 years old. The depth of the olfactory fossae was categorized according to Keros classification, and the location of the AEA was then determined.

The olfactory fossa depth ranged from 0.8 to 9.1 mm. Keros type II was the most common (72.8 % & 77.8 %) of male and female patients, respectively, without statistically significant gender difference. The AEA location was asymmetric in 48.7%. A significant correlation was found between AEA running beneath the skull and higher Keros type. About two-thirds of the studied Iraqi adult population showed asymmetric olfactory fossa depth with nearly half of AEA running below the skull base; therefore, Iraqi radiologists and Ear–Nose–Throat surgeons should be aware of this anatomical variation to avoid serious surgical complications**.**

Keywords: Ethmoid Bone; Helical Computerized tomography; Paranasal Sinuses; Skull Base;

Introduction

The ethmoid bone consists of three parts: the cribriform plate, labyrinths, and perpendicular plate. The paper-thin cribriform plate represents the nasal cavity roof (Pedro Monterio et al; 2017) and the olfactory fossa (OF) floor, which is bounded medially by the crista Galli and laterally and by the lateral lamella of the cribriform plate (LLCP)(Vaid et al. et al; 2015). Keros develop a system for the OF depth classification by measuring the maximum LLCP height. Keros type I is assigned when the depth is less than or equal to 3 mm, 4–7 mm is considered type II while >7 mm represents type III (Nair et al; 2012). Since the paranasal sinuses' size and shape are of the most variable structures (Lorkiewicz-Muszyńska et al. et al; 2015), the ethmoid roof height may be asymmetric in the same individual (Reddy et al. et al; 2012).

The anterior ethmoidal artery (AEA) is an ophthalmic artery branch with intraorbital, ethmoidal, and intracranial segments(Chaisiwamongkol et al; 2012). Before it enters the olfactory fossa after piercing the lateral lamella then it crosses the anterior ethmoid sinus roof (Alsaied et al; 2017), running either within a bony canal at the skull base 'non-hanging' or hanging below the skull base with dehiscence of the AEA bone covering is reported in up to 90% of cases(Zinreich et al. et al; 2019). It represents a critical structure within the ethmoid sinus which possesses a great risk of iatrogenic injury (Bortoli et al. et al; 2017); thus, surgical manipulations must be limited to its level (Yang et al. et al; 2009). When injured, the AEA may continue to bleed inside the orbit causing orbital hematoma which necessitates decompression otherwise decreased visual acuity or even amaurosis will result (Ferrari et al. et al; 2017).

The ability to diagnose and appropriately manage sinus disease has dramatically improved by cross-sectional imaging(Kandukuri et al. et al; 2016). The minimally invasive functional Endoscopic Sinus Surgery (FESS) (Tajudeen et al. et al; 2017) manages PNS pathologies such as inflammatory and neoplastic conditions. Despite being safer than the traditional approaches (Adeel et al. et al; 2013), most of the major complications like CSF leakage, meningitis, and ocular or intracranial vascular traumatization are related to the ethmoid bone(Kaplanoglu et al. et al; 2013).

Various factors such as lateral lamella configuration, AEA path, and asymmetry of olfactory fossa depth are important anatomic variations in FESS (Jacob et al. et al; 2014). Since these anatomic variations are extremely wide, the surgical planning is preferably tailored preoperatively with the aid of a CT scan rather than relying solely on the standard intraoperative landmarks(Nair et al; 2012, Jang et al. et al; 2014). There is a great disparity in the contents of the preoperative sinus CT imaging report (Deutschmann et al. et al; 2013), and to our best knowledge, there is no published article precisely assessing the olfactory fossae Keros classification and AEA location to the skull base in Iraqi people. This study was conducted to clarify the regional anatomical variations regarding these structures, which enable the radiologist to clearly understand the anatomy of the ethmoid roof and to include this surgically relevant information in their CT reports. Since the included patients are not only from Baghdad governorate's cities but from different governorates, the study assumes to represent the Iraqi population.

Materials and Methods

This hospital-based cross-sectional observational study involves 189 patients (90 males, 99 female) in the Al-Yarmouk teaching hospital CT unit, Baghdad, Iraq. Patients referred to the radiology department for the evaluation of sinonasal diseases and examined by non-contrast CT scan using paranasal sinuses protocol were included. Patients <18 years of age and those with altered anatomy due to congenital anomalies of the face, trauma, previous sinonasal surgery, neoplasm or diseases that interfere with accurate measurement weren't included.

Data acquisition: relevant demographic and clinical data (age, presenting complaint, and previous history of trauma or surgery, etc.) were obtained. The CT scan of each patient was evaluated in the following approach:

1. Assessment to rule out any exclusion criteria.
2. The ethmoidal roof was evaluated in the PNS window of coronal reformatted CT. The LLCP height was measured between a superior point at the medial aspect of the ethmoid roof and an inferior point at the cribriform plate, and its vertical height corresponds to the OF depth. The left and right lateral lamellae heights were separately recorded, the OF depth in this study was classified according to Keros classification(Keros et al; 1962) as follows: Keros I: 1 to 3.99 mm deep, Keros II: 4 to 7.99 mm deep, Keros III: ≥ 8 mm deep.
3. The course of the AEA was identified based on the following anatomical landmarks: the anterior ethmoid foramen which is a notch on the medial orbital wall or the anterior ethmoid sulcus on the OF lateral wall. The AEA course was identified on either side separately and classified as being within or separate from the skull base and it was seen fully or partially. In the case of being hanging from the skull, the distance between them was measured vertically at the midpoint of its course.

Statistical analysis: data analysis was carried out using SPSS version 22 software. Categorical variables are presented as absolute numbers and percentages. Categorical variables were analyzed with Pearson's chi-squared test and Fisher's exact test. Continuous data were expressed as Mean ±SD. Comparison of continuous variables was analyzed using an Independent Sample T-test and ANOVA tests according to several independent variables and if the data is normally distributed. If the data is not normally distributed, differences between groups were examined by a nonparametric test. The correlation between continuous variables was measured by Pearson test if the data is normally distributed. A P-value of less than 0.05 was considered significant.

Results

The 254 paranasal CT scans were reviewed and 65 scans were excluded as they met the exclusion criteria. Of the 189 studied patients, there was 99 female (52.38%) and 90 male (47.62 %). The mean age of them was 32.5 ±11.4 years. For each patient, both sides were independently assessed, and each side was considered to be a single measurement for analysis, a total of 378 ethmoidal roofs & AEAs were studied.

The depth of the olfactory fossae ranged from 0.8 to 9.1 mm, no significant association exists between gender and olfactory fossa depth on either side (table 1). Asymmetric OF depth was observed in 62.4% of patients, with a difference in the OF depth between the two sides equal or more than 0.1 mm was considered asymmetric (figure 1). Among 118 subjects with asymmetric OF depth, 64.6% had a difference of ≤1 mm, 24.5% 1–2 mm difference, and 11.1% showed a difference of more than 2 mm between two sides. The patient gender and the symmetry of OF depth show no significant association (table 2). Keros type II was the most common (75.4%) in all studied age groups without a significant association between the patient age, gender, and Keros type on both sides (table 3and 4). Among 189 subjects, 86.8 % showed the same Keros type on both sides without a significant association between gender and the symmetry of Keros type on both sides (table 5).

The AEA location to the skull on both sides was summarized in (Table 6) with a significant association between the mean distance of AEA from the skull base & Keros type on the RT side (table 7). The AEA status was asymmetric (being within the skull base on one side & below it on the other side) in 48.7% of patients without a statistically significant relationship between gender &AEA location symmetry (table 8, figure 2, 3, and 4). While less than 10% of those with Keros type I had hanging AEA, nearly half of those with Keros type III showed hanging artery thus, a significant correlation between AEA being below the skull base and higher Keros type was found (table 9). There was a positive (P-value = 0.007) weak (R= 0.214) correlation between the olfactory fossa depth and the frequency with which the AEA was below skull base on both sides. This significant correlation indicates that increase the olfactory fossa depth is associated with increased AEA distance below the skull base.

Discussion

To our knowledge, no dedicated in-depth study had been done to evaluate the anterior ethmoidal artery distance from skull base & olfactory fossa depth in Iraq; therefore, the results were thoroughly compared with the published studies in other countries. In this study, the mean OF depth was (4.7±1.6)mm in males and (4.6 ±1.5)mm in females, while in Babu et al. (Babu et al. et al; 2018), its depth was (5.3± 1.7, 5.1 ±1.6)mm in males and females, respectively. Asymmetric olfactory fossa depth was seen in 62.45% of cases (61.1% of male and 63.6% of female) with 64.6% had ≤1 mm difference between two sides, 1–2 mm difference was seen in 24.5%, and 11.1% showed more than 2 mm difference, 73.7% had deeper right OF while in Babu et al. (Babu et al. et al; 2018) 75% of their patients showed asymmetric OF depth without significant difference among both genders (75.8% of males and 74% of females) with (64.6%) had a difference of ≤1 mm, and 10.1% had more than 2 mm difference between two sides, 51.3% had deeper right OF, in Satish Nair(Nair et al; 2012)11.7% had asymmetry(71.4% had deeper right OF) and in Ali et al. (Ali et al. et al; 2005) 14.6% of patients had asymmetry(63.6% had deeper right OF). In a previous study conducted in Iraq(Aliasghar et al. et al; 2016), asymmetrical ethmoidal roofs were noted in 3.4% of their patients without a clear explanation for their definition of "asymmetry "or detailed analysis of the OF depth and Keros type. The higher percentage of asymmetry noted in the current study & in Babu et al. (Babu et al. et al; 2018) may be attributed to the more strict definition of asymmetry.

Keros type II was the most frequent in the current study. This finding was similar to those reported elsewhere, such as in Turkey (Ahmet et al. et al; 2018, Kaplanoglu et al. et al; 2013, Şahin et al. et al; 2007, Erdem et al. et al; 2004), Saudi Arabia (Alrumaih et al. et al; 2016), Egypt (Elwany et al. et al; 2010), Brazil(Souza et al. et al; 2009), Australia(Floreani et al. et al; 2006), Mexico(Muñoz-Leija et al. et al; 2018), Pakistan (Adeel et al. et al; 2013), Thailand(Nitinavakarn et al. et al; 2005), Kashmir(Salroo et al. et al; 2016), India(Babu et al. et al; 2018, Nair et al; 2012, Jacob et al. et al; 2014, Ali et al. et al; 2005, Pawar et al. et al; 2017, Gupta et al. et al; 2017)and USA (Poteet et al. et al; 2017); however other studies showed that type I is the most common such in Egypt (Shama et al. et al; 2015), Nepal(Bista et al. et al; 2010), Philippines (Paber et al. et al; 2008), USA(Solares et al. et al; 2008), Malaysia(Alazzawi et al. et al; 2012), UK(Nouraei et al. et al; 2009) and Jordan(Athamneh et al. et al; 2015)while type III was the most common in Gauba et al.(UK)(Gauba et al. et al; 2006). These wide variations (tables 10) can be attributed to the diversity in olfactory fossa configuration among the different populations or the sample size & the non-balanced age distribution. For example among the reviewed studies, Bista et al.(Bista et al. et al; 2010) sample was the smallest (i.e., 50 CT scans). However different results were noticed even among studies performed on the same race like Shama et al (Shama et al. et al; 2015) and Elwany et al(Elwany et al. et al; 2010)(both were conducted among the Egyptian population) which may relate to the size of the studied sample, measurement methods, and the standardization regarding the measurements (more than three and less than four as well as more than seven and less than 8 mm) which wasn’t originally described (Sakandar et al. et al; 2019).

A different Keros type on either side was seen among (13.2%) of our patients, in (Pawar et al. et al; 2017, Babu et al. et al; 2018) this was found in 11.5%, 21.7%, respectively, without statistically significant association between olfactory fossa depth, Keros type, and gender or side, this finding also noted by costa (Costa et al. et al; 2019), salroo(Salroo et al. et al; 2016). In (Güldner et al. et al; 2012), two groups of patients were assessed (i.e., those younger and those older than 18 years) and observed that Keros type I was the most common in the former; while, Keros type II was the most common in the latter. To some extent, the current findings are following their results. On the contrary, OF depth on both sides differs significantly in Erdogan et al. (Erdogan et al. et al; 2015), Murthy(V et al. et al; 2017), Sarı H(Sari et al. et al; 2017), and Alazzawi(Alazzawi et al. et al; 2012), the association between gender and Keros type was statistically significant in Babu et al.(Babu et al. et al; 2018)

About (41 %) of the anterior ethmoid arteries run below the skull with a mean distance of (4 ±1.45)mm on the right side and (4.02±1.36) mm on the left side, while in another study, the percentage of hanging AEA was 12.5%(Monjas-Cánovas et al. et al; 2011), 16.7(Simmen et al. et al; 2006), 25.7%(Poteet et al. et al; 2017), and 37.3% (Abdullah et al. et al; 2019). A symmetric AEA location was seen in 48.7% of our patients (53.3% of male & 44.4% of female) without a statistically significant association between gender and AEA location symmetry. In (Costa et al. et al; 2019)the average distance between the AEA midpoint to the skull was 3.85 mm on the left side and 3.18 mm on the right and about 4% of patients had asymmetric AEA course. These different results may be caused by the analysis method, racial and climate differences, and their effect on craniofacial development (Kim et al. et al; 2010). A significant correlation was there between the AEA course inferior to the skull base and the higher Keros type. This finding was also noted in (Poteet et al. et al; 2017) where the AEA was below the skull with a greater frequency with higher Keros type (0% in Keros type I, 29.5% Keros type II and 55% Keros type III).

The Limitations of this work include:

1. The clinical setting does not represent the daily clinical practice where trauma, inflammatory changes, and disease processes would be expected to change the skull base anatomy and alter the analytical perception of the radiologists.
2. All CT scans of those aged less than 18 years old were intentionally excluded from the analysis, therefore, care should be taken when applying the findings of this study to the general population.

Conclusion: about two-thirds of the studied Iraqi adult population showed asymmetric olfactory fossa depth with nearly half of AEA running below the skull base therefore, Iraqi radiologists and Ear–Nose–Throat surgeons should be aware of this anatomical variation to avoid serious surgical complications.

References

- Abdullah, B., Et Al. 2019. Anatomical Variations Of Anterior Ethmoidal Artery At The Ethmoidal Roof And Anterior Skull Base In Asians. Surg Radiol Anat, 41, 543-550.
- Adeel, M., Et Al. 2013. Asymmetry Of Lateral Lamella Of The Cribriform Plate: A Software-Based Analysis Of Coronal Computed Tomography And Its Clinical Relevance In Endoscopic Sinus Surgery. Surgical And Radiologic Anatomy, 35, 843-847.
- Ahmet, S., Et Al. 2018. Sex-Related Changes In The Configuration Of The Ethmoid Roof And Evaluation Of Asymmetry. Ec Clinical And Experimental Anatomy, 1, 83-92.
- Alazzawi, S., Et Al. 2012. Radiological Analysis Of The Ethmoid Roof In The Malaysian Population. Auris Nasus Larynx, 39, 393-6.
- Ali, A., Et Al. 2005. Anterior Skull Base: High Risk Areas In Endoscopic Sinus Surgery In Chronic Rhinosinusitis: A Computed Tomographic Analysis. Indian Journal Of Otolaryngology And Head And Neck Surgery, 57, 5-8.
- Aliasghar, A., Et Al. 2016. Co-Existence Of Anatomical Variants And Rhinosinusitis On Multi-Sliced Computed Tomography. Iraqi Postgraduate Medical Journal, 15.
- Alrumaih, R. A., Et Al. 2016. Radiological Sinonasal Anatomy: Exploring The Saudi Population. Saudi Medical Journal, 37, 521.
- Alsaied, A. S. 2017. Paranasal Sinus Anatomy: What The Surgeon Needs To Know, Intechopen.
- Athamneh, I., Et Al. 2015. Keros Classification Among Jordanian Population. Journal Of The Royal Medical Services, 22, 69-72.
- Babu, A. C., Et Al. 2018. Olfactory Fossa Depth: Ct Analysis Of 1200 Patients. The Indian Journal Of Radiology & Imaging, 28, 395.
- Bista, M., Et Al. 2010. Computed Tomographic Assessment Of Lateral Lamella Of Cribriform Plate And Comparison Of Depth Of Olfactory Fossa. Jnma J Nepal Med Assoc, 49, 92-5.
- Bortoli, V. T., Et Al. 2017. Study Of Anthropometric Measurements Of The Anterior Ethmoidal Artery Using Three-Dimensional Scanning On 300 Patients. International Archives Of Otorhinolaryngology, 21, 115-121.
- Chaisiwamongkol, K. 2012. Landmark Of Ethmoid Arteries In Adult Thai Cadavers: Application For Sinus Surgery. J Med Assoc Thai, 95, S153-S156.
- Costa, A. L. F., Et Al. 2019. Cone Beam Computed Tomography-Based Anatomical Assessment Of The Olfactory Fossa. Int J Dent, 2019, 4134260.
- Deutschmann, M. W., Et Al. 2013. Radiologic Reporting For Paranasal Sinus Computed Tomography: A Multi-Institutional Review Of Content And Consistency. The Laryngoscope, 123,

1100-1105.
- Elwany, S., Et Al. 2010. Radiological Observations On The Olfactory Fossa And Ethmoid Roof. The Journal Of Laryngology & Otology, 124, 1251-1256.
- Erdem, G., Et Al. 2004. A Radiological Anatomic Study Of The Cribriform Plate Compared With Constant Structures. Rhinology, 42, 225-9.
- Erdogan, S., Et Al. 2015. Ethmoid Roof Radiology; Analysis Of Lateral Lamella Of Cribriform Plate. Otolaryngol Pol, 69, 53-7.
- Ferrari, M., Et Al. 2017. The Ethmoidal Arteries: A Cadaveric Study Based On Cone Beam Computed Tomography And Endoscopic Dissection. Surgical And Radiologic Anatomy, 39, 991-998.
- Floreani, S. R., Et Al. 2006. Endoscopic Anterior Ethmoidal Artery Ligation: A Cadaver Study. The Laryngoscope, 116, 1263-1267.
- Gauba, V., Et Al. 2006. Radiological Classification Of Anterior Skull Base Anatomy Prior To Performing Medial Orbital Wall Decompression. Orbit, 25, 93-6.
- Güldner, C., Et Al. 2012. Age-Dependent Differences Of The Anterior Skull Base. Int J Pediatr Otorhinolaryngol, 76, 822-8.
- Gupta, P., Et Al. 2017. Radiological Observation Of Ethmoid Roof On Basis Of Keros Classification And Its Application In Endonasal Surgery. International Journal Of Approximate Reasoning, 5, 4204-4207.
- Jacob, T. G., Et Al. 2014. Morphology Of The Olfactory Fossa – A New Look. Journal Of The Anatomical Society Of India, 63, 30-35.
- Jang, D. W., Et Al. 2014. Supraorbital Ethmoid Cell: A Consistent Landmark For Endoscopic Identification Of The Anterior Ethmoidal Artery. Otolaryngology–Head And Neck Surgery, 151, 1073-1077.
- Kandukuri, R., Et Al. 2016. Evaluation Of Sinonasal Diseases By Computed Tomography. Journal Of Clinical And Diagnostic Research: Jcdr, 10, Tc09.
- Kaplanoglu, H., Et Al. 2013. An Analysis Of The Anatomic Variations Of The Paranasal Sinuses And Ethmoid Roof Using Computed Tomography. The Eurasian Journal Of Medicine, 45, 115.
- Keros, P. 1962. On The Practical Value Of Differences In The Level Of The Lamina Cribrosa Of The Ethmoid. Zeitschrift Fur Laryngologie, Rhinologie, Otologie Und Ihre Grenzgebiete, 41, 809-813.
- Kim, J., Et Al. 2010. Comparative Study Of The Pneumatization Of The Mastoid Air Cells And Paranasal Sinuses Using Three-Dimensional Reconstruction Of Computed Tomography Scans. Surg Radiol Anat, 32, 593-9.
- Lorkiewicz-Muszyńska, D., Et Al. 2015. Development Of The Maxillary Sinus From Birth To Age 18. Postnatal Growth Pattern. International Journal Of Pediatric Otorhinolaryngology, 79, 1393-1400.
- Monjas-Cánovas, I., Et Al. 2011. [Radiological Anatomy Of The Ethmoidal Arteries: Ct Cadaver Study]. Acta Otorrinolaringol Esp, 62, 367-74.
- Muñoz-Leija, M. A., Et Al. 2018. Anatomical Variations Of The Ethmoidal Roof: Differences Between Men And Women. European Archives Of Oto-Rhino-Laryngology, 275, 1831-1836.
- Nair, S. 2012. Importance Of Ethmoidal Roof In Endoscopic Sinus Surgery. Sci Rep, 1, 1-3.
- Nitinavakarn, B., Et Al. 2005. Anatomical Variations Of The Lateral Nasal Wall And Paranasal Sinuses: A Ct Study For Endoscopic Sinus Surgery (Ess) In Thai Patients. J Med Assoc Thai, 88, 763-8.
- Nouraei, S. A., Et Al. 2009. Variations In Paranasal Sinus Anatomy: Implications For The Pathophysiology Of Chronic Rhinosinusitis And Safety Of Endoscopic Sinus Surgery. J Otolaryngol Head Neck Surg, 38, 32-7.
- Paber, J. E. L. B., Et Al. 2008. Radiographic Analysis Of The Ethmoid Roof Based On Keros Classification Among Filipinos. Philippine Journal Of Otolaryngology Head And Neck Surgery, 23, 15-19.
- Pawar, A., Et Al. 2017. Assessment Of Depth Of Olfactory Fossa In Pre-Functional Endoscopic Sinus Surgery Computed Tomography Scan Of Paranasal Sinuses. 2017, 4, 4.
- Pedro Monterio, D. L. 2017. Endoscopic Ethmoidectomy _Fess_ Surgical Technique. Open Access Atlas Of Otolaryngology, Head &
- Neck Operative Surgery.
- Poteet, P. S., Et Al. 2017. Analysis Of The Relationship Between The Location Of The Anterior Ethmoid Artery And Keros Classification. Otolaryngol Head Neck Surg, 157, 320-324.
- Reddy, U. D. M. A., Et Al. 2012. Pictorial Essay: Anatomical Variations Of Paranasal Sinuses On Multidetector Computed Tomography-How Does It Help Fess Surgeons? The Indian Journal Of Radiology & Imaging, 22, 317.
- Şahin, C., Et Al. 2007. Analysis Of Ethmoid Roof And Cranial Base In Turkish Population. Kbb Ve Bbc Dergisi, 15, 1-6.
- Sakandar, G., Et Al. 2019. Adult And Pediatric Lateral Lamella Cribriform Plate Height: In Need For A Comparative Study. Allergy Rhinol (Providence), 10, 2152656719874775.
- Salroo, I. N., Et Al. 2016. Computerised Tomographic Profile Of Ethmoid Roof On Basis Of Keros Classification Among Ethnic Kashmiri's. Int J Otorhinolaryngol Head Neck Surg, 2, 1-5.

- Sari, H., Et Al. Importance Of Keros Classification In Surgery. 2017.
- Shama, S. A., Et Al. 2015. Variations Of The Height Of The Ethmoid Roof Among Egyptian Adult Population: Mdct Study. The Egyptian Journal Of Radiology And Nuclear Medicine, 46**,** 929-936.
- Simmen, D., Et Al. 2006. The Surgeon's View Of The Anterior Ethmoid Artery. Clin Otolaryngol, 31**,** 187-91.
- Solares, C. A., Et Al. 2008. Lateral Lamella Of The Cribriform Plate: Software-Enabled Computed Tomographic Analysis And Its Clinical Relevance In Skull Base Surgery. Arch Otolaryngol Head Neck Surg, 134**,** 285-9.
- Souza, S. A., Et Al. 2009. Anterior Ethmoidal Artery Evaluation On Coronal Ct Scans. Brazilian Journal Of Otorhinolaryngology, 75**,** 101-106.
- Tajudeen, B. A., Et Al. 2017. Thirty Years Of Endoscopic Sinus Surgery: What Have We Learned? World Journal Of Otorhinolaryngology-Head And Neck Surgery, 3**,** 115-121.
- V, A. M., Et Al. 2017. A Study Of Clinical Significance Of The Depth Of Olfactory Fossa In Patients Undergoing Endoscopic Sinus Surgery. Indian J Otolaryngol Head Neck Surg, 69**,** 514-522.
- Vaid, S., Et Al. 2015. Normal Anatomy And Anatomic Variants Of The Paranasal Sinuses On Computed Tomography. Neuroimaging Clinics, 25**,** 527-548.
- Yang, Y.-X., Et Al. 2009. Morphological Characteristics Of The Anterior Ethmoidal Artery In Ethmoid Roof And Endoscopic Localization. Skull Base, 19**,** 311-317.
- Zinreich, S., Et Al. 2019. Advanced Ct Imaging Demonstrating The Bulla Lamella And The Basal Lamella Of The Middle Turbinate As Endoscopic Landmarks For The Anterior Ethmoid Artery. Rhinology Online, 7**,** 32-43.

The Tables

table 1: association of olfactory fossa depth in both sides with gender

Gender	*Right side OF depth	****P-value*	*Left side OF depth	****P-value*	***mean OF depth
Male	4.8±1.678	0.749	4.69±1.54	0.25	4.75±1.6
Female	4.88±1.50		4.44±1.5		4.66±1.55

* Measured in mm

** Independent sample T test

*** Both right and left side involved

table 2: distribution of symmetric and asymmetric of depth on either side according to gender

Gender	Asymmetric	Symmetric	Total	**P value*
Male	55**(46.6)	35 (49.3)	90(47.6)	0.072
Female	63 (53.4)	36 (50.7)	99(52.4)	
total	118(100)	71(100)	189(100)	

* Pearson Chi-Square

**Values between brackets are percentages.

table 3: association of Keros type and age group on both sides of the skull

Age (years)	Right side			*P-value*	Left side			*P-value*
	type I	type II	type III		type I	type II	type III	
18-27	8 (25.8)	54 (39.1)	7 (35)	0.266	8 (26.7)	56 (38.1)	4 (33.3)	0.601
28-37	11(35.5)	43 (31.2)	3 (15)		9 (30)	47 (32)	2 (16.7)	
38-47	9 (29)	25 (18.1)	9 (45)		10(33.3)	27 (18.4)	5 (41.7)	
48-57	3 (9.7)	9 (6.5)	1 (5)		2 (6.7)	11 (7.5)	1 (8.3)	
58-67	0	6 (4.3)	0		1 (3.3)	5 (3.4)	0	
68-77	0	1 (0.7)	0		0	1 (0.7)	0	
Total	31 (100)	138(100)	20(100)		30 (100)	147(100)	12 (100)	

*Fisher's exact test

table 4: distribution of Keros classification according to the side and gender

Keros type	Right side		*P value*	Left side		*P value*	***Total	
	male	female		male	female		male	female
I	17**(18.9)	14(14.1)	0.476	14(15.5)	16(16.1)	0.744	31(17.2)	30 (15.1)
II	62(68.9)	76(76.8)		69(76.7)	78(78.8)		131(72.8)	154(77.8)
III	11(12.2)	9 (9.1)		7 (7.8)	5 (5.1)		18 (10)	14 (7.1)

* Pearson Chi-Square
**Values between brackets are percentages.
*** Both right and left sides involved

table 5: distribution of subjects with same and different keros types on either side according to gender

Gender	Keros type on both side		Total	*P-value*
	Asymmetrical	Symmetrical		
Male	16 **(17.8)	74 (82.2)	90 (100)	0.078
Female	9 (9.1)	90 (90.9)	99 (100)	

* Pearson Chi-Square
**Values between brackets are percentages.

table 6: distribution of anterior ethmoidal artery location to skull base on both side

AEA location	Right side	Left side
below	77 *(40.7)	79(41.8)
within	112 (59.3)	110(58.2)
Total	189(100)	189(100)

* Values between brackets are percentages.

Table 7: The mean distance of the AEA from the skull base to the Keros type on each side.

Keros type	the mean distance of the AEA from the skull base*			
	Right side	***P value*	Left side	*P value*
type I	3.8±0.28	**< 0.0001**	3.9±0.98	0.159
type II	3.7±1.16		3.94±1.34	
type III	5.6±1.91		4.97±1.45	
Total	4±1.45		4.02±1.36	

*Measured in mm
**One-Way ANOVA

Table 8: Distribution of symmetric and asymmetric AEA location to the skull base in both gender

Gender	Asymmetrical	Symmetrical	Total	**P value*
Male	48 **(53.3)	42 (46.7)	90 (100)	0.222
Female	44 (44.4)	55 (55.6)	99 (100)	
Total	92 (48.7)	97 (51.3)	189 (100)	

*Pearson Chi-Square
**Values between brackets are percentages.

Table 9: Correlation of the frequency of AEA location to the skull base with Keros classification

Keros class	**AEA location to the skull base***		**total no.**	****P-value***
	below	**within**		
I	6 ***(9.8)	55 (90.2)	61 (100)	**< 0.0001**
II	131 (46)	154 (54)	285 (100)	
III	19 (59.4)	13 (40.6)	32 (100)	
Total No.	156 (41.3)	222 (58.7)	378 (100)	

*Both sides were considered
**Pearson Chi-Square
***Values between brackets are percentages.

Figures

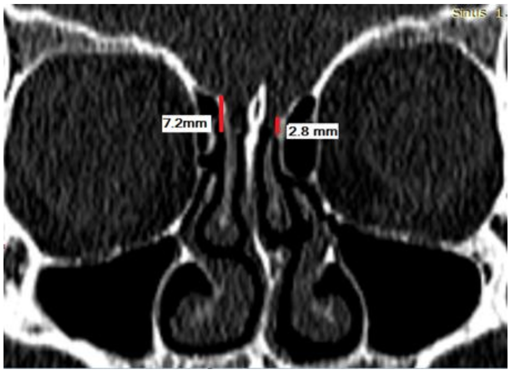

Fig. 1: coronal CT scan shows asymmetric OF (Keros I on the left and III on the right)

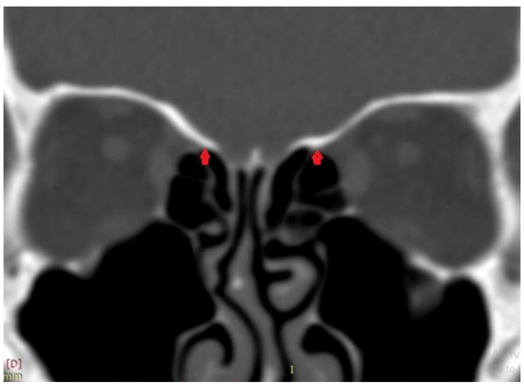

Fig. 2: coronal CT scan shows anterior ethmoidal artery (arrow) located within the skull base on both sides

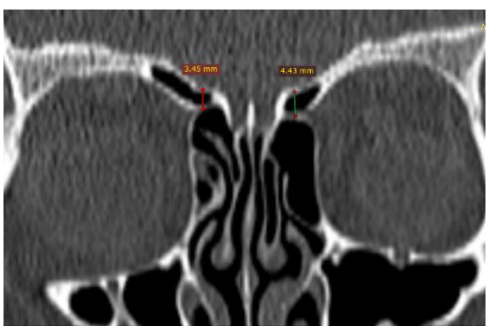

Fig. 3 coronal CT scan: AEA hanging below the skull (distance given in millimeter)

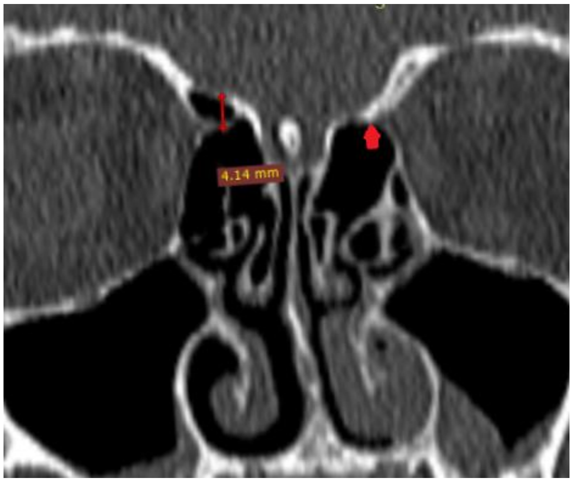

Fig. 4 coronal CT scan: AEA located below the skull on the right and within it on the left (arrow)